Coordination Chemistry Reviews 254 (2010) 781–793

Contents lists available at ScienceDirect

Coordination Chemistry Reviews

journal homepage: www.elsevier.com/locate/ccr

Review

Model systems for the CO-releasing flavonol 2,4-dioxygenase enzyme

József Sándor Pap, József Kaizer*, Gábor Speier

Department of Chemistry, Universtiy of Pannonia, 8201 Veszprém, Hungary

Contents

ARTICLE INFO

Article history:
Received 15 September 2009
Accepted 11 November 2009
Available online 11 December 2009

Keywords:
Bioinorganic chemistry
CO-releasing dioxygenases
Flavonol
Copper
Biomimetic oxygenation

ABSTRACT

In this review structural and reactivity studies on the co-ligand containing model complexes for the flavonol 2,4-dioxygenase (FDO) are covered. The main focus is on the relationship between the structural features of the copper-containing model complexes, and their activity in the enzyme-like reactions. Some radical initiated reactions and catalytic systems will also be discussed.

1. Introduction

Flavonoids are polyphenolic pigments found in higher plants and some fungi [1]. Numerous representatives such as quercetin (3,5,7,3′,4′-pentahydroxyflavone) are well known for their antioxidant and antimicrobial properties [2]. Being present in many fruits and vegetables, these species provide an important source of antioxidant and antibacterial dietary supplement for humans. With the degradation of the plant material, however, microbicidal flavonoids get into the soil, too, where bacteria and fungi are exposed to these compounds. In response, soil microorganisms have developed effective catabolic systems utilizing flavonoids as a carbon source with the help of flavonol 2,4-dioxygenase (FDO) enzymes, which can transform flavonoids into the corresponding depsides (phenolic carboxylic acid esters) under aerobic conditions (1) [3–6]. In addition to the incorporation of both atoms of molecular oxygen into the organic substrate molecule (normal dioxygenase function), the FDO catalysed oxygenation of flavonol derivatives involves the cleavage of two carbon–carbon bonds, and the concomitant production of carbon monoxide according to Eq.

* Corresponding author. Tel.: +36 88 62 4720; fax: +36 88 62 4469.
E-mail address: kaizer@almos.vein.hu (J. Kaizer).

0010-8545/$ – see front matter © 2009 Elsevier B.V. All rights reserved.
doi:10.1016/j.ccr.2009.11.009

(1) [7]. Not surprisingly, these metalloenzymes have drawn much attention in the last decades.

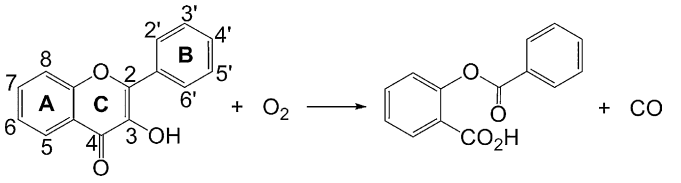

(1)

Quercetinases were first isolated and most extensively studied from *Aspergillus* species, *A. flavus* [8], *A. niger* [6] and *A. japonicus* [9]. These were all characterised as highly glycosylated bicupin proteins binding type II copper ion at the active site. Bacterial FDO enzymes with different cofactors have also recently been isolated, but will not be further discussed here [10,11]. Our present review focuses on the functional and structural model systems related to the fungal copper-containing native FDOs. First we give a brief overview of the studies on the enzymatic reaction and the structure of the enzymatic active site from *A. japonicus*. A more detailed insight will be presented into the mechanistic details of the oxygenation reactions carried out with model substrates. We provide a thorough understanding of the influence of metal and ligand moieties as well as those of the substrate coordination modes on the reaction mechanism.

2. Fungal flavonol 2,4-dioxygenase enzymes

2.1. Structure of the enzymatic active site

Although FDO enzymes had been spectroscopically investigated before, the real breakthrough was the structural characterisation of the enzyme from *A. japonicus* [9]. The enzyme is described as a homodimer containing one copper(II) ion per monomer unit. The 1.6 Å resolution crystal structure of this ~100 kDa molecular weight dimeric glycoprotein reveals that the active site is found in a cavity ~10 Å from the protein surface, and is solvent exposed. In the apoenzyme, there are two alternative coordination forms for the copper ion in accordance with electron paramagnetic resonance (EPR) observations. In form A (Fig. 1) the copper is ligated by three hystidine residues and by a water molecule in a distorted tetrahedral geometry. This form is present in 70% in the native enzyme and gives the major $g_{||}$ signal at 2.330 and with $A_{||}$ = 13.7 mT in the X-band EPR spectrum [12]. Form B (Fig. 1) represents a trigonal bipyramidal coordination mode and is present in nearly 30% giving the minor EPR signal ($g_{||}$ = 2.290 and $A_{||}$ = 12.5 mT). In this case an additional glutamate is bound to the copper that puts the water molecule further away from the copper site. Carboxylate coordination to a native copper-containing active site is unique and as will be discussed later, has a crucial role in the catalytic activity.

2.2. Structure of the enzyme-substrate (ES) complex

It has been clear since the early studies that the number and distribution of the hydroxyl functions on the substrates has a great influence on the reactivity [13] resulting in varying reaction rates for their oxygenation. Apart from the effect of the hydroxyl functions on the intrinsic reactivity of the substrate [14], hydrogen bonding between these functions (in the 3′, 4′, 5, or 7 positions, see Eq. (1)) and the peptide residues (tyrosine and threonine) found near the active site, positions the flavonol derivatives to the copper site with different orientation, and plays an important role in the substrate-dependent reactivity. For instance, hydroxyl groups on the C7 and C3′ atoms of quercetin result in a faster oxidation rate whereas hydroxyl substitution on the C8 atom slows down the oxidation dramatically. Manual modelling of the substrate coordination at the active site revealed that the most reactive quercetin, partly due to the above-mentioned interactions, is very likely bound as a monodentate ligand via the 3-hydroxyl group displacing the water molecule from the coordination sphere. Further structural information on the ES complex was deduced from the structural analysis of FDO crystallised with kojic acid as ligand on the metal [12]. This study showed that similarly to form B of the enzyme, the glutamate remains bound to the copper site after the formation of the ES complex (Fig. 2) and probably plays a role in substrate deprotonation. However, in contrast to flavonol derivatives, which are bound in a monodentate fashion, kojic acid chelates the copper ion in FDO through its hydroxyl (O3) and carbonyl oxygen (O4) atoms. Further evidence for the coordination mode of the ES complex was provided based on EXAFS experiments on anaerobic complexes of FDO with quercetin and myricetin (5′-hydroxyquercetin) [15]. The copper environment is five-coordinate, and is best modelled by a single shell of N/O scatterers, approximately 2.00 Å from the metal, also an indication of the monodentate substrate coordination.

2.3. Mechanism of the enzymatic reaction

General questions regarding the function of dioxygenases include the number of oxygen molecules involved in the reaction and the order and mechanism of activation of the reactants (*i.e.* substrate and O_2) at the active site. The oxidation of flavonol derivatives is often paralleled with the catabolism of haem (degradation

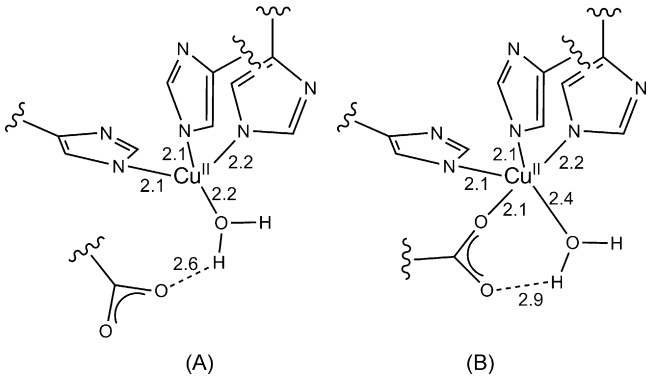

Fig. 1. Coordination modes of copper in the FDO active site from *A. japonicus*. Distances indicated in the scheme are in (Å).

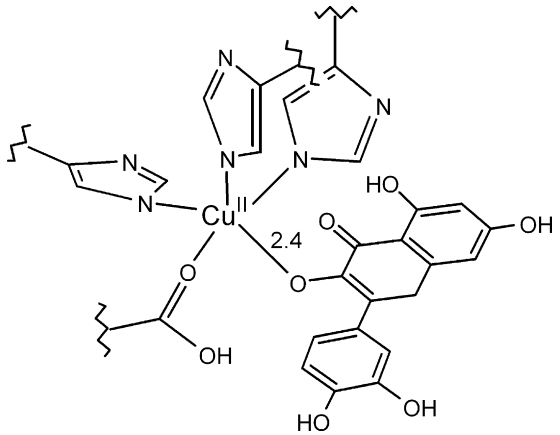

Fig. 2. X-ray crystal structure (at 1.6 Å resolution) of the quercetin-enzyme complex (The Cu–O distance is in (Å)).

of haem into biliverdin via hydroxyhaem formation). A major difference, however, is that while haem undergoes a two-molecule mechanism, during which the oxygen atoms that are incorporated into the substrate originate from two dioxygen molecules, FDO utilizes only one dioxygen molecule per substrate (one-molecule mechanism) that was proven by mass spectral analysis of the reaction product by FDO in a mixture of $^{18}O_2$ and $^{16}O_2$ [16]. The order of activation was understood via studying the anaerobic ES complexes [17] and some mechanistic information was obtained from EPR experiments [18]. The results indicate that the first step in the enzymatic process is the binding of the flavonol derivative as a monodentate ligand to the copper site. This step does not require the presence of dioxygen, *i.e.* the substrate activation step precedes the oxidation of the metal site as shown in Scheme 1. After formation of the ternary ESO_2 complex oxygenation of the substrate takes place and CO is released before the depside leaves the site. Some of these steps are further supported by studies on model reactions (*vide infra*).

Another intriguing question is the place of dioxygen attack on the ES complex. The generally accepted presumption is, that

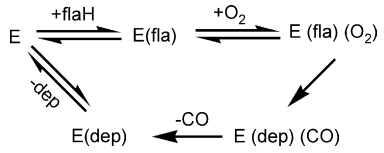

Scheme 1.

an ES_{rad} valence isomer is formed which can react with $^3O_2$ in two ways as is shown in Fig. 3 (path a and b). Although some hybrid DFT calculations [19] indicate that the energetically preferred one is b, others do not exclude path a [20] as an alternative. Geometrical considerations based on the crystal structures of ES complexes [17] also support the latter pathway.

Although the experiments on native enzymes answered some fundamental questions, some remained unresolved. These include the activation mode of the coordinated flavonolate (coordinated anion *vs.* radical formation) and the possible role of glutamate function coordinated to copper. Model reactions and complexes

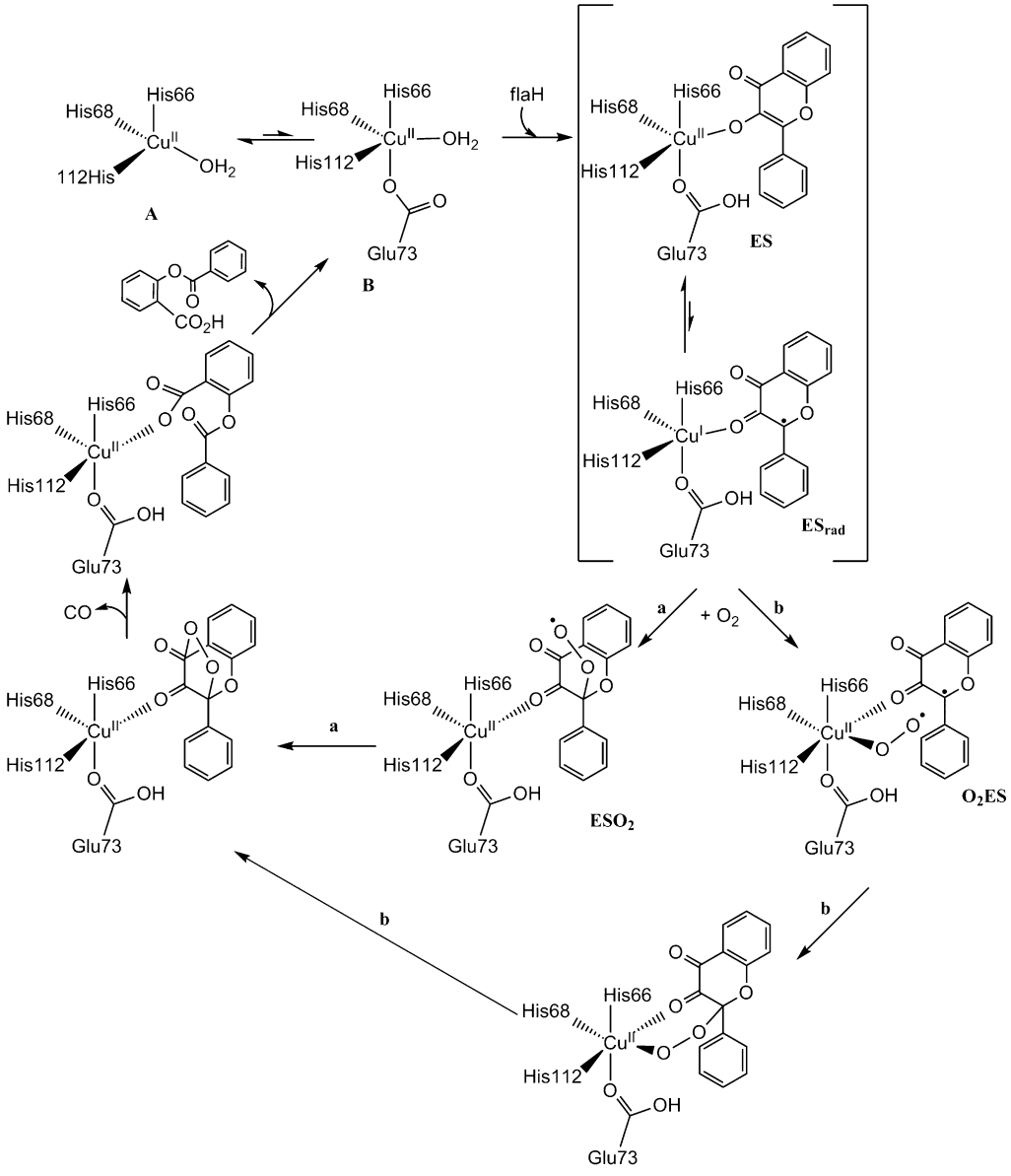

Fig. 3. Proposed mechanism for the enzymatic oxygenation of flavonols (from ref. [11]).

that are discussed in the next chapters aim to elucidate such problems.

3. Model systems

Early studies involved simple base-catalysed [21–23] and photosensitised reactions [24] of quercetin and related compounds with dioxygen as well as direct reactions of flavonol with superoxide [25] as models for the enzymatic process. The fact, on the other hand, that the FDO enzymes employ a copper cofactor early shifted attention to elucidate the possible role of this redox-active metal during the enzymatic oxygenation process with the help of copper(I)- and copper(II)-containing flavonolato-complexes that have been directly oxygenated, or tried as catalysts in the oxygenation of the substrate. Conclusions based on such model systems and non-redox metal assisted systems have been discussed in a recent review [26], and will be mentioned only briefly. In the next chapters we present an overview of model complexes and reactions involving N- and O-donor ligands, focusing on the spectroscopic and structural properties of the formers in connection with the mechanistic aspects of the latter.

3.1. Base-catalysed and non-redox metal assisted oxygenation of flavonols

These reactions are carried out either under aqueous [21] or non-aqueous [21,22] conditions. In both cases dioxygen reacts with the substrate analogously to the enzymatic reaction and in addition to the enzymatic product depside, hydrolysed secondary products were identified. Formation of the enzymatic products was rationalised by assuming that 2-hydroperoxyflavan-3,4-dionate anion is formed first according to Eq. (2).

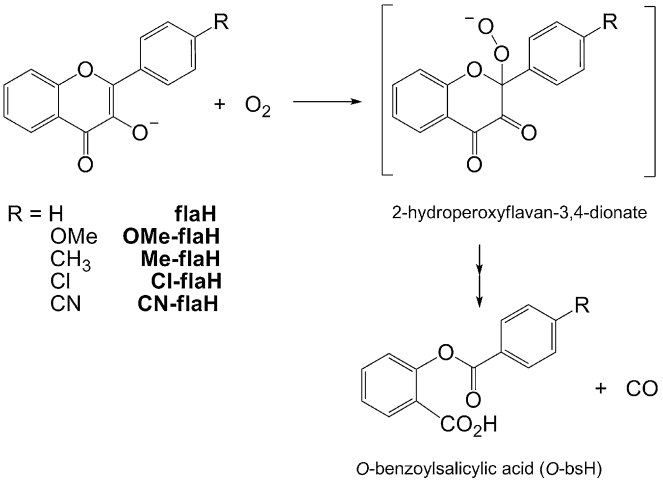

(2)

A more detailed mechanistic study was carried out with flavonol and its 4′-substituted derivatives (see also Eq. (2)) in a 50% DMSO–water solvent mixture [27]. The reaction showed specific base catalysis and fits a Hammet linear free energy relationship for the 4′-substituted derivatives ($\rho = -0.50$). The latter indicates higher electron density on the C ring of the flavonol (*i.e.* more electron donating substituents) that makes the electrophilic attack of O_2 easier, an indication for the potential of the deprotonated substrate to reduce triplet dioxygen directly. The reactivity of potassium flavonolate derivatives in aprotic medium was also studied [23]. The presence of a flavonoxy radical presumes a single electron transfer (SET) mechanism in which again, the anionic substrate reduces the triplet dioxygen, which then provides the enzymatic product via recombination and formation of a putative 2-hydroperoxyflavan-3,4-dionate intermediate species as seen in Eq. (2). A similar mechanism is proposed for the oxygenation of a zinc-containing model complex with the 3N-donor 3,3′-iminobis(*N,N*-dimethylpropylamine (idpa, see Fig. 4) [28]. In this case the formation of superoxide radical anion is observed with nitroblue tetrazolium (NBT) test [28] suggesting a SET mechanism. Recombination of the presumable zinc-bound flavonoxy radical and the superoxide radical anion results in a transient peroxide-species, which then decomposes into the enzymatic product. The bimolecular rate equation and the negative activation entropy ($-96 \pm 1\,J\,mol^{-1}\,K^{-1}$) [28] support the above associative mechanism. As in the case of the base-catalysed oxygenations, electron-releasing groups on the substrate make the reaction rate faster. Summarily: non-redox metal assisted oxygenolysis of flavonol derivatives in aprotic solvents has a single electron transfer (SET) mechanism in which the substrate with increased basicity reduces the molecular oxygen, initiating further steps that lead to the enzyme-like product.

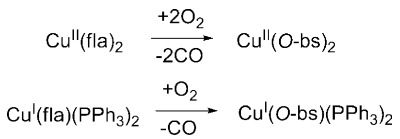

Scheme 2.

3.2. Copper-containing models for the enzyme-substrate (ES) and enzyme-product (EP) complexes

The reactivity of the copper(II)–flavonolate binary complex and the copper(I)–triphenylphosphine–flavonolate ternary complex [29–31] was studied and discussed in the earlier review [26]. Both complexes mime the enzyme action and provide the corresponding *O*-benzoylsalycilate complexes as oxygenation products (Scheme 2), but with a surprisingly low rate. Since the key feature of the copper(II) flavonolate complex is that the flavonols coordinate as a chelate to the copper centre, this is thought to be the main reason for the lower reaction rate compared to that of the enzyme. It is further indicated by the accelerating effect of added pyridine [32] that competes with the flavonolate ligand for the sites thus forcing monodentate flavonolate coordination.

Thus, we may presume that application of ligands in model complexes that are bound to the copper centre, and model the enzymatic metal binding site, might result in better structural models for the ES complex, as well as better functional models. We have prepared several complexes along this line of thought using the ligands seen in Fig. 4, which made it possible to draw conclusions from the reactivity–structure relationships.

3.2.1. Structural features of the co-ligand containing copper(II) flavonolate (ES model) complexes

All complexes have been characterised by IR and UV–vis spectroscopy and some with X-ray crystallography. Coordination of the substrates flaH and mcoH (Fig. 3) to the copper site is indicated by the characteristic ν_{CO} band between 1540 and 1580 cm^{-1} (Table 1, see also there for references). Compared to that of the ν_{CO} vibration at 1610 cm^{-1} of free flavonol [33] this band is shifted by 30–70 cm^{-1} to lower energies. This can be interpreted by the formation of a stable five-membered chelate that is formed upon the coordination of the 3-OH and 4-CO oxygen atoms of the flavonol and partially populates the π^* antibonding orbital of the carbonyl group *via* back-donation from copper d orbitals. In the UV–vis absorption spectrum the bathochromic shift of the flavonol π–π^* transition from ~340 nm to 420–440 nm shows unambiguously the presence of

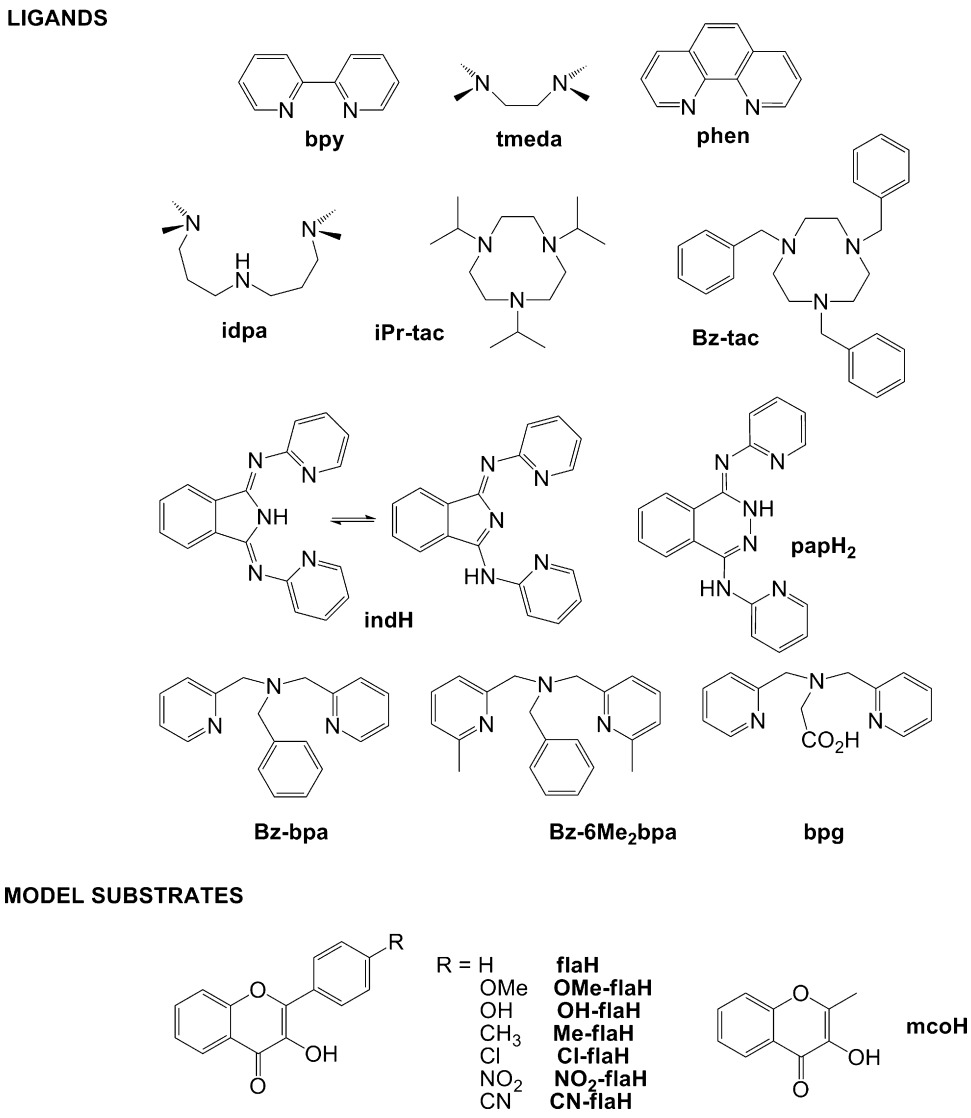

Fig. 4. Applied ligands and model substrates with their abbreviated names.

Table 1
IR and UV–vis spectroscopy data for the studied ES complexes.[a].

Complex	IR[b], ν_{CO}(cm^{-1})	UV–vis[c], λ (nm) ($\log \varepsilon_{max}$)	Ref.
[Cu(fla)(idpa)]ClO_4	1559	732 (2.31); 427 (3.99)	[34]
[Cu(fla)(*i*Pr-tac)]ClO_4	1554	1065 (1.89); 653(2.15); 434 (3.52)	[35]
[Cu(Bz-tac)(fla)]ClO_4	1545	1040 (1.73); 615(2.90); 432 (2.23)	[35]
[Cu(Bz-bpa)(fla)]ClO_4	1541	421 (4.13)	[36]
[Cu(Bz-6Me_2bpa)(fla)]ClO_4	1545	429 (4.09)	[36]
[Cu(bpg)(fla)]	1543	421 (4.32)	[36]
[Cu(ind)(mco)]	1577	618 (1.87); 450 (4.43) 423 (4.49)	[37]
[Cu(fla)(ind)]	1574	631 (2.18); 444 (3.96) 415 (4.17)	[38]
[Cu(fla)(phen)$_2$]ClO_4	1581	702 (1.71); 419 (3.92)	[39]
[Cu(fla)$_2$(phen)]	1564	674 (2.58); 426 (4.75)	[39]
[Cu(bpy)(fla)$_2$]	1578	431 (4.77)	[39]
[Cu(fla)$_2$(tmeda)]	1573	674 (2.58); 430 (4.78)	[39]
[Cu(fla)(MeCN)(tmeda)]ClO_4	1545	623 (1.50); 427 (4.27)	[40]
[Cu(bpy)(fla)(ClO_4)]	1540	637 (2.30); 427 (4.26)	[41]
[Cu(fla)$_2$]	1536	426 (4.56) 410 (4.53)	[32]

[a] Structures of the abbreviation ligands are shown in Fig. 4.
[b] In KBr.
[c] In DMF solution at room temperature.

the coordinated substrate (Table 1). Bands at lower energies (600–700 nm) originate from the d–d transitions of the copper(II) ions.

Crystal structures of the complexes (Fig. 5) further support the bidentate coordination of flavonol that leads to the formation of a very stable five-membered chelate ring in each case. All the applied co-ligands are 3N-donors, thus the copper site is five-coordinated with distorted geometry. The extent of distortion from the ideal trigonal bipyramidal (TBPY) or square pyramidal (SPY) arrangement ($\tau = 0$ in an ideal TBPY complex and $\tau = 1$, in case of an ideal SPY arrangement) is highly influenced by the 3N-donor ligand. As seen from Table 2, the τ parameter embraces a wide range ($\tau = 0.12–0.71$).

The structures of the Cu(fla)(L) model complexes studied differ from that of the enzymatic active site regarding the substrate coordination mode: bidentate coordination is experienced in the models in all cases, whereas in the enzyme only the 3-enolate function is bound to the metal. This difference can be explained by means of van der Waals forces and H-bonding that prohibit the formation of the otherwise thermodynamically favoured five-membered chelate ring. These secondary interactions are ruled out in the case of our synthetic models.

On the other hand, changes in the geometry of the five-coordinate copper complexes will influence the electron delocal-

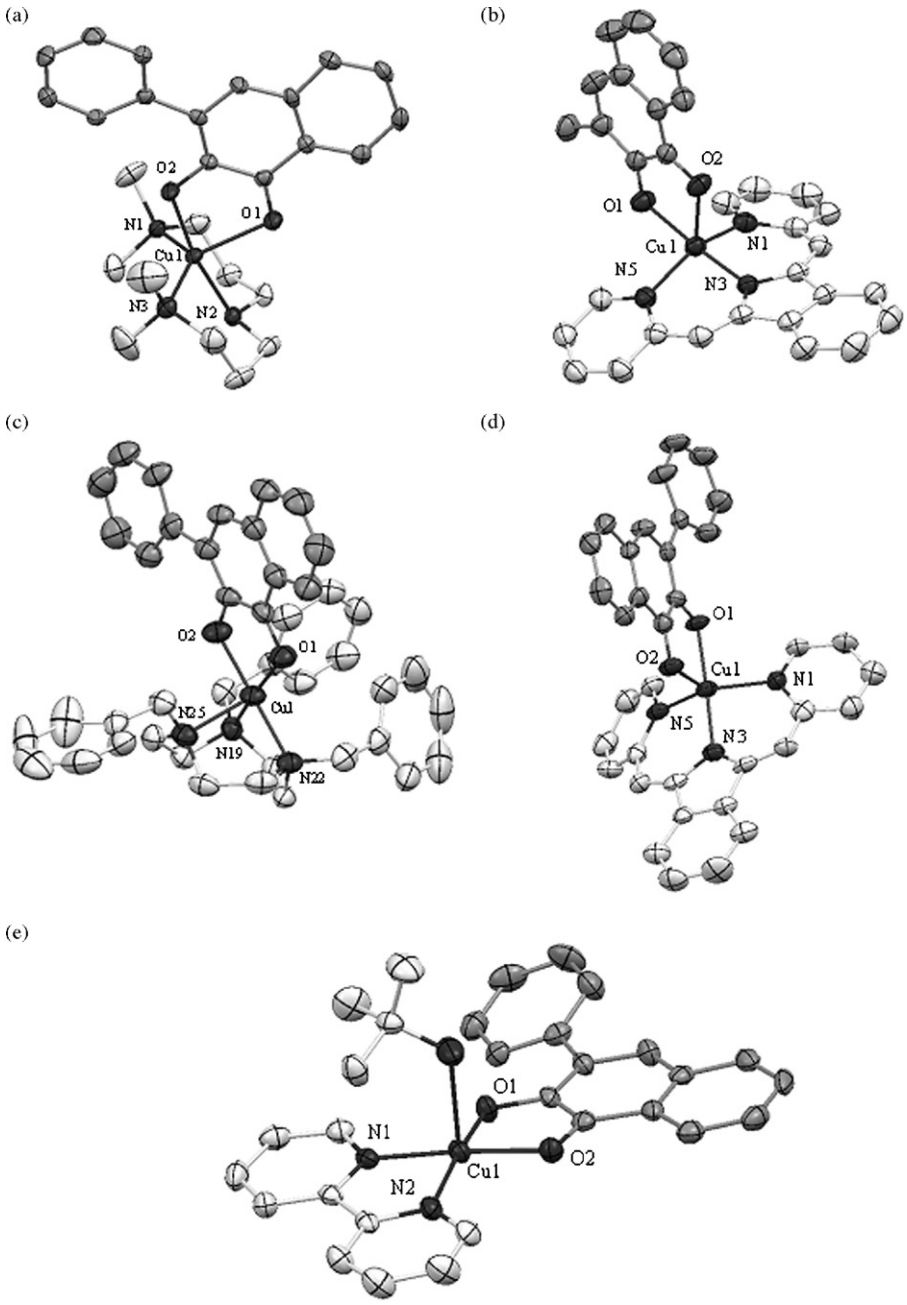

Fig. 5. X-ray structure of some synthetic ES complexes: [Cu(fla)(idpa)]ClO_4 (a); [Cu(ind)(mco)] (b); [Cu(Bz-tac)(fla)]ClO_4 (c); [Cu(fla)(ind)] (d); [Cu(bpy)(fla)ClO_4] (e). Thermal ellipsoids are at 50% probability level.

isation, and thus the bond distance between the copper centre and the flavonolate oxygen atoms. While in SPY geometries the $Cu–O_{enolate}$ and the $Cu–O_{keto}$ bond lengths are nearly equidistant, in complexes with TBPY geometry this Δ value approaches 0.3 Å. If the difference between the Cu–O bond distances is plotted against the τ value, correlation becomes clear (Fig. 6). As will be seen in Section 3.3.2, distortion of the Cu–fla chelate will considerably change the reaction rate of the oxygenation of model complexes.

3.2.2. Structural features of the co-ligand containing copper(II) O-benzoylsalicylate (EP model) complexes

Synthetic enzyme-product (EP) complexes can be prepared directly, or by reacting the corresponding ES complex with dioxygen. The EP complexes have been structurally characterised (X-ray diffraction, IR and UV–vis spectroscopy). The relevant spectroscopic and structural data are given in Table 3 (IR, UV–vis; see references) and Table 4 (X-ray).

The ν(CO) bands for the ester bond in the infrared spectrum of the EP complexes remain unchanged compared to the corresponding value for the free *O*-benzoylsalicylic acid (*O*-bsH). As a consequence, this moiety does not take part in the ligation. The value of the ν_{as}(CO) and ν_s(CO) bands for the *O*-bs^- carboxylate function, on the other hand provides us information on the coordination mode. The difference between the energy of the symmetric and asymmetric stretching modes allows us to predict the mono-, or bidentate coordination mode of the carboxylate moiety to the copper. X-ray diffractional structures (where available) are in good accordance with this IR-based estimation.

Table 2
Structural data for synthetic ES type complexes.[a].

Complex		Bond distance (Å)[b]	Δ (Å)[c]	τ	Ref.
[Cu(fla)(idpa)]ClO_4	Cul–O1 Cul–O2	2.210 (3) 1.918 (3)	0.292	0.61	[34]
[Cu(ind)(mco)]	Cul–O1 Cul–O2	1.9506 (14) 2.2966 (14)	0.347	0.38	[37]
[Cu(Bz-tac)(fla)]ClO_4	Cu–O1 Cul–O2	1.917 (3) 2.012 (3)	0.095	0.12	[35]
[Cu(fla)(ind)]	Cul–O1 Cul–O2	1.942 (5) 2.206 (6)	0.264	0.50	[38]
[Cu(bpy)(fla)(ClO_4)]	Cul–O1 Cul–O2	1.971 (3) 2.897 (3)	0.074	0.10	[41]

[a] Structures of the abbreviation ligands are shown in Fig. 4.
[b] See Fig. 5 for relevant atom numbering.
[c] |(Cul-O1)–(Cul–O2)|.

Formation of the EP complexes can be followed by UV–vis spectrophotometry in cases where we oxygenate the precursor ES complexes, since the π–π* charge transfer band that is characteristic for the flavonolate ligand, disappears. Thus UV–vis spectroscopy becomes a useful tool in the kinetic investigations of the ES complex oxygenation reactions.

Among the X-ray crystallographically characterised compounds (Fig. 7), we can find examples for the bidentate *O*-bs$^-$ coordination (a, b, c and d) and for the monodentate (e, f and g) as well. Bond distances and bond angles are found in Table 4. With increasing of the $\nu_{as}(CO)-\nu_s(CO)$ difference the $\Delta(Cu-O_{carboxylate})$ value shows a linear increase with a good correlation (Fig. 8). In other words, a relatively big difference between the $\nu_{as}(CO)$ and $\nu_s(CO)$ indicates monodentate coordination mode for the *O*-bs$^-$ ligand. Of the EP models, compounds with TBPY geometry describe structurally correctly the native enzyme-product complex. Based on the available data [Cu(bpg)(*O*-bs)] ($\tau = 0.51$) is the best structural model so far.

3.3. Functional models for flavonol 2,4-dioxygenase

Studies on the FDO enzymes implied that the substrate coordination and concomitant activation at the active site makes the oxidative decarbonylation of quercetin viable. Early model reactions involving ES type complexes, however, took place at reasonable rate typically only at higher temperatures (80–120 °C). At such high thermal energy levels the initial activation of dioxygen instead of that of the substrate remains an alternative mechanism. To elucidate the order of substrate *vs.* dioxygen activation $EO_2 + S$

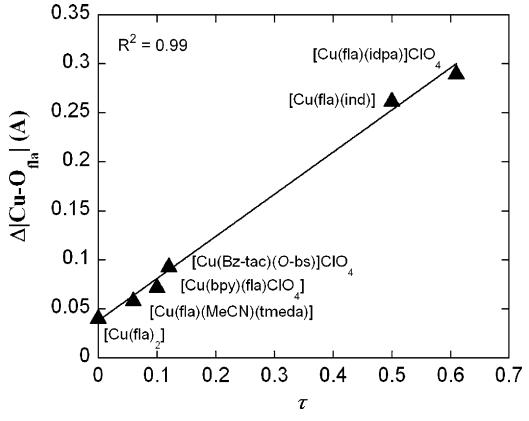

Fig. 6. The π-electron delocalisation in flavonolate ligand in correlation with the geometry of the Cu(L)(fla) complexes.

Table 3
IR and UV–vis data for EP complexes.[a].

Complex	IR[b] (cm^{-1}) $\nu_{as}(CO)$, $\nu_s(CO)$	UV–vis[c], λ (nm) (log ε_{max})	Ref.
[Cu(idpa)(*O*-bs)]ClO_4	1572,1375	716(2.45); 276(3.98)	[34]
[Cu(*i*Pr-tac)(*O*-bs)]ClO_4	1584,1428	1060(1.73); 670(1.43); 278 (3.23)	[35]
[Cu(Bz-tac)(*O*-bs)]ClO_4	1586,1432	1065 (1.62); 650 (1.96); 276 (3.81)	[35]
[Cu(Bz-bpa)(*O*-bs)]ClO_4	1559,1374	682 (2.41); 270 (3.85)	[36]
[Cu(Bz-6Me_2bpa)(*O*-bs)(ClO_4)]	1570,1375	736 (2.16); 271 (3.93)	[36]
[Cu(bpg)(*O*-bs)]	1571,1344	914 (1.50); 270 (3.72)	[36]
[Cu(ind)(*O*-bs)]	1578,1380	816 (1.17); 447 (3.97); 272 (4.04) 421 (4.04) 334 (4.02) 309 (4.02)	[38]
[Cu(asp)(H_2O)(ind)]	1531,1357	662 (213); 446 (4.29); 272 (4.30) 421 (4.35) 335 (4.27) 312 (4.28)	[37]
[Cu(*O*-bs)(phen)$_2$]ClO_4	1572,1388	684 (2.06); 331 (3.31); 294 (4.25)	[39]

[a] Structures of the abbreviation ligands are shown in Fig. 4.
[b] In KBr.
[c] In DMF solution at room temperature.

type reactions were carried out with the known copper(II)- and copper(III)-dioxygen adducts, [{Cu^{III}(Bz-tac)}$_2$(μ-O)$_2$](ClO_4) and [{Cu^{II}(*i*Pr-tac)}$_2$(μ-η^2:η^2-O)$_2$](ClO_4)$_2$, and flavonol [43–45]. The reaction yields only the corresponding ES type complexes, excluding the dioxygen activation pathway as shown in Scheme 3 [35].

Mechanistic details for some model systems have been discussed in earlier reviews [26,46]. Studies summarised therein highlight the redox-role of the copper centre, the electronic effect of the substituents on the flaH moiety and the influence of the N-ligands on the chemoselectivity. While some complexes follow the enzymatic reaction pathway ([Cu(fla)$_2$] and [Cu(fla)(PPh_3)$_2$]) during oxygenation, others deviate from it producing no carbon monoxide, but different oxygenation products ([Cu(fla)$_2$(tmeda)], [Cu(bpy)(fla)$_2$] and [Cu(fla)$_2$(phen)]). The proposed overall mechanism is shown in Scheme 4 for the two pathways found in model systems. Apart from major differences, a common feature is that both involve a pre-equilibrium between the copper(II) flavonolate and its proposed valence tautomer copper(I) flavonoxy radical complex. The flavonoxy radical is thought to be very unstable, which is

Table 4
Selected structural data for the EP complexes.[a].

Complex		Bond distance (Å)[b]	τ	Ref.
[Cu(idpa)(*O*-bs)]ClO_4	Cul–O1 Cul–O2	1.995 (5) 2.344 (9)	0.16	[34]
[Cu(Bz-tac)(*O*-bs)]ClO_4	Cu–O1A Cu–O2A	1.9772 (17) 2.0685 (19)	0.16	[35]
[Cu(*i*Pr-tac)(*O*-bs)]ClO_4	Cul–O1 Cul–O2	1.981 (6) 2.020 (7)	0.10	[35]
[Cu(Bz-6Me_2bpa)(*O*-bs)(ClO_4)]	Cul–O1	1.9835 (19)	–	[36]
[Cu(bpg)(*O*-bs)]	Cul–O1 Cul–O3	1.972 (2) 2.015 (2)	0.51	[36]
[Cu(*O*-bs)(phen)$_2$]ClO_4	Cul–O1	1.993 (4)	0.47	[39]
[Cu(H_2O)(ind)(sal)]	Cul–O24 Cul–O1	2.0053 2.4344	0.25	[42]

[a] Structures of the abbreviation ligands are shown in Fig. 4.
[b] See Fig. 7 for relevant atom numbering.

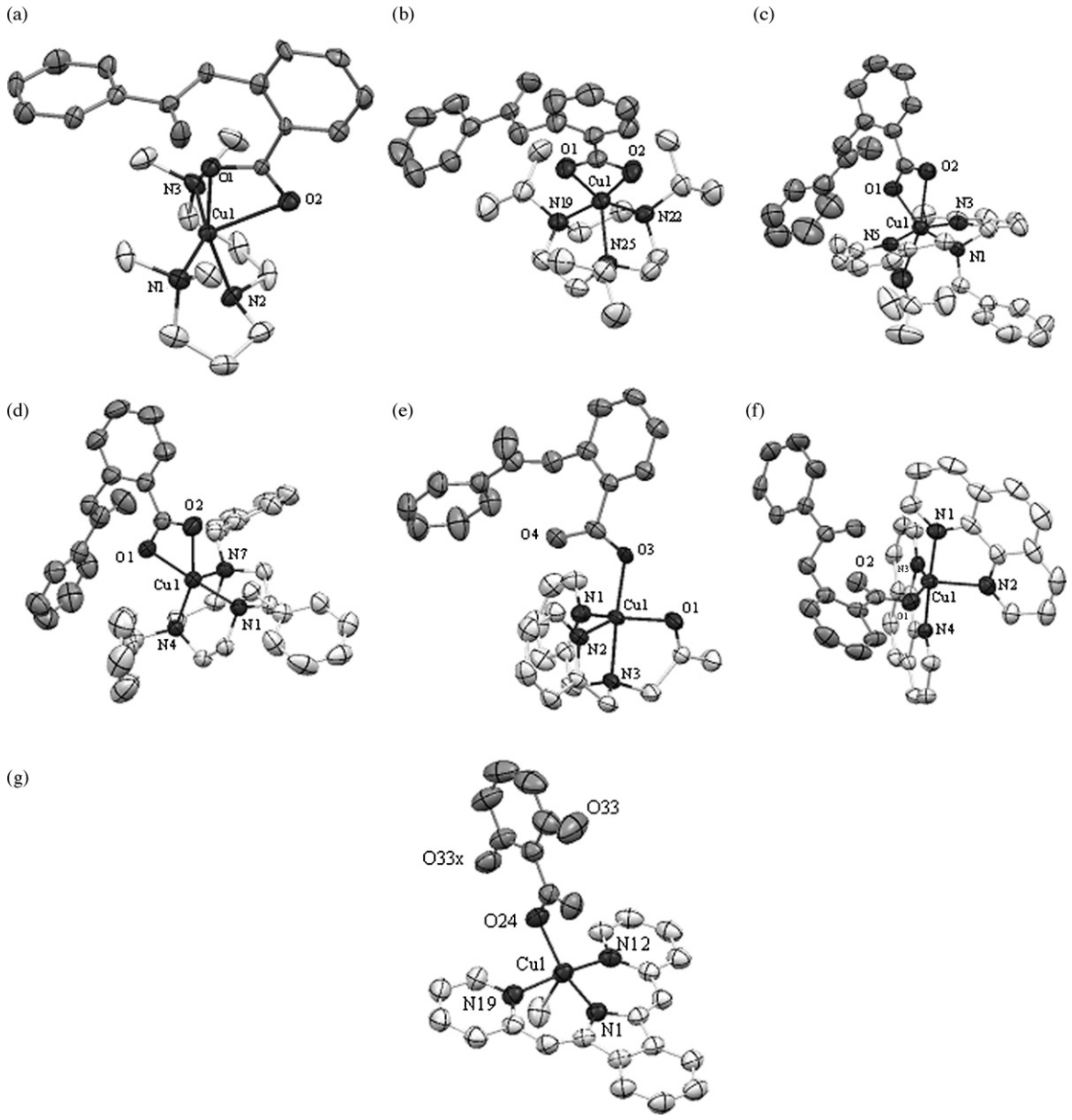

Fig. 7. X-ray structure of the EP complexes: [Cu(idpa)(*O*-bs)]ClO_4 (a); [Cu(Bz-tac)(*O*-bs)]ClO_4 (b); [Cu(*i*Pr-tac)(*O*-bs)]ClO_4 (c); [Cu(Bz-6Me$_2$bpa)(*O*-bs)(ClO_4)] (d); [Cu(bpg)(*O*-bs)] (e); [Cu(*O*-bs)(phen)$_2$]ClO_4 (f); [Cu(asp)(H_2O)(ind)] (g).

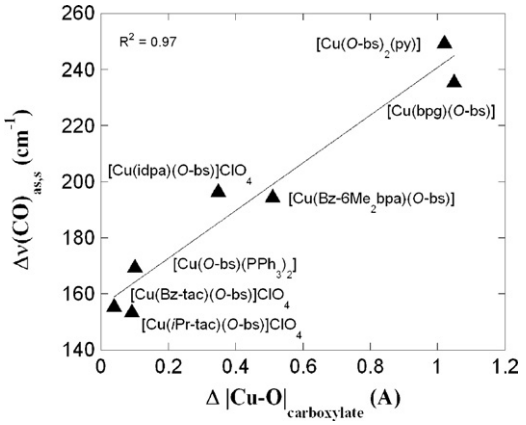

Fig. 8. Carboxylate coordination mode for *O*-bs$^-$. Correlation between the energy difference of the IR stretching bands of the carboxylate function and the copper–carboxylate oxygen bond distance differences.

supported by its difficult preparation, and poor detection in EPR. When bound to copper(I), this radical is somewhat stabilised and potentially can react with the triplet dioxygen bound to the copper centre, or vice versa, it can bind $^3O_2$, which then attacks the copper centre. Here we focus on the nature and reactivity of the flavonoxy radical and further factors that influence the reaction rate, namely the geometry of the ES complexes and the application of carboxylate co-ligands. Substrate specificity will also be shown.

3.3.1. *Radical initiated oxygenation of flavonol*

One-electron oxidation of flavonol derivatives leads to the formation of the unstable flavonoxy radical (Scheme 5). This reaction can be facilitated by using outer sphere one-electron oxidant (cerium(IV) ammonium nitrate, CAN), or a stable radical initiator like TEMPO (2,2,6,6-tetramethylpiperidinyloxy free radical). Under an inert atmosphere the generated radical forms a dehydro-dimer (Scheme 5 and Fig. 9, b), that is bound via the 3-O (Scheme 5, A) of one flavonoxy and the 2-C (Scheme 5, B) atom of the other flavonoxy radical demonstrating the spin delocalisation in the rad-

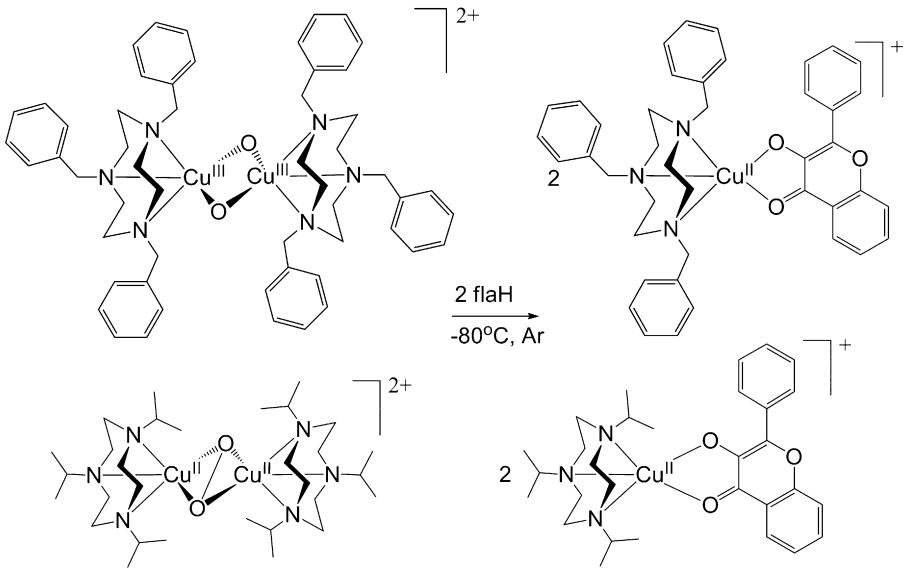

Scheme 3.

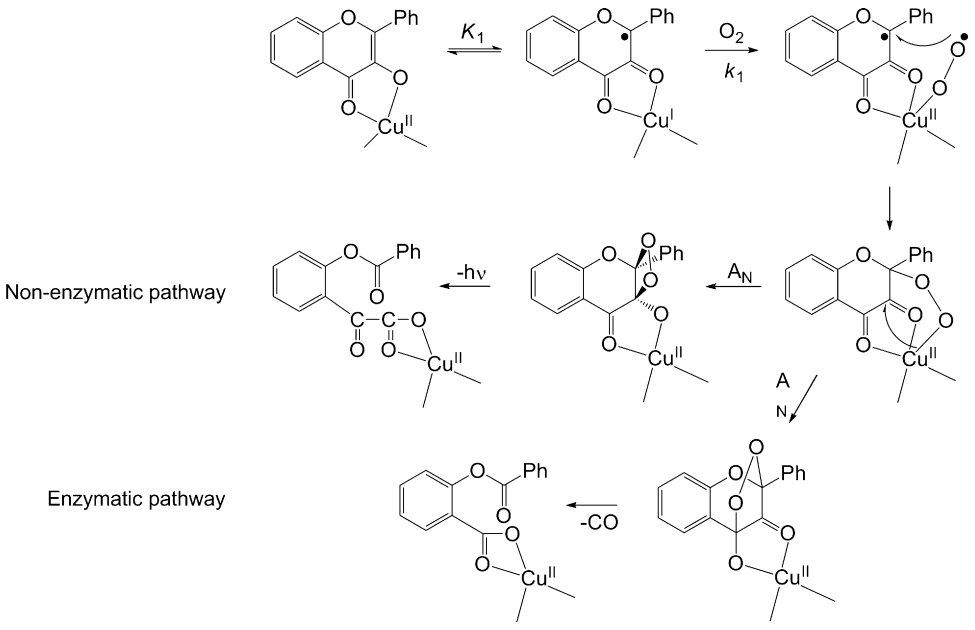

Scheme 4.

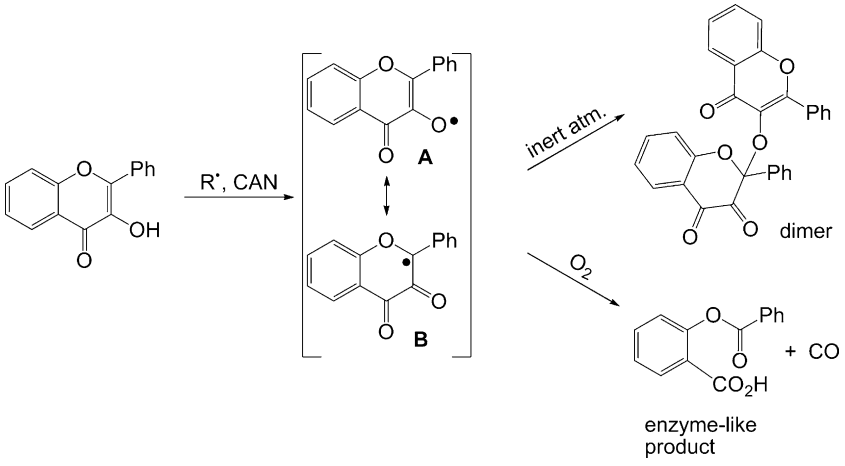

Scheme 5.

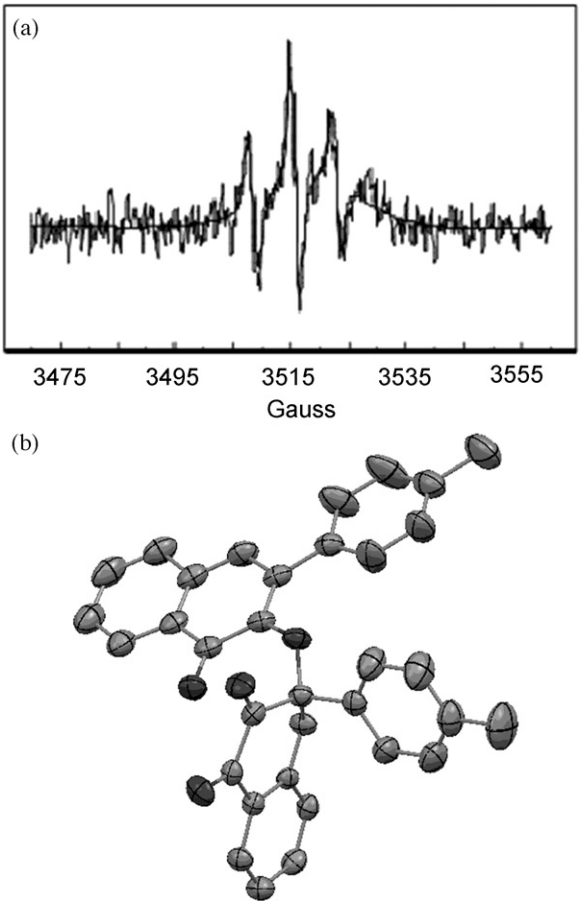

Fig. 9. (a) EPR spectrum of the flavonoxy radical: ($a_{H(1)}$ = 8.1; $a_{H(1)'}$ = 6.4; $a_{H(2)''}$ = 1.08 G; g = 2.0067). (b) Crystal structure of the dehydro-dimer.

ical [47]. The weak EPR signal (Fig. 9, a) of the sample from the Me–flaH reaction with CAN is a resolved triplet where the shape of lines indicates two slightly different major and two non-resolved additional coupling processes. This can be attributed unambiguously to the oxygen-centred radical, whereas no signal could be assigned to the 2-C centred radical. DFT calculations showed that from the three possible radical–radical coupling combinations this one is the most thermodynamically and sterically favoured (bond energies are C–O = 79 kcal/mol and O–O = 34 kcal/mol) [47].

Oxidation of the radical follows the enzymatic pathway producing *O*-benzoylsalicylic acid and CO [48]. In the presence of Galvinoxyl (2,6-di-*tert*-butyl-α-(3,5-di-*tert*-butyl-4-oxo-2,5-cyclohexadien-1-ylidene)-*p*-tolyloxy, free radical), or TEMPO, the oxidation is slow, only high temperature, or an electron pushing substituent on the B ring promotes the reaction. Accordingly, highest yields were obtained with Me–flaH at 70 °C in MeCN.

2,2-Diphenyl-1-picryl-hydrazyl (DPPH) as initiator reacts with flaH already at room temperature. Kinetic measurements revealed a bimolecular rate equation with partial orders of one for the flaH and the DPPH. The rate-determining step thus is the flavonoxy radical formation, which is followed by its fast reaction with $^3O_2$ giving *O*-bsH as product.

In the enzyme and in the model systems (a) $^3O_2$ attack can take place on the 2-C carbon atom of the flavonoxy radical, besides its rather likely attack on the copper(I) centre as is shown in Fig. 3 and (b) the flavonolate ligand is rich enough in energy to be able to give up one electron to $^3O_2$ yielding a superoxide anion representing an alternative pathway for the enzyme-like reaction. The

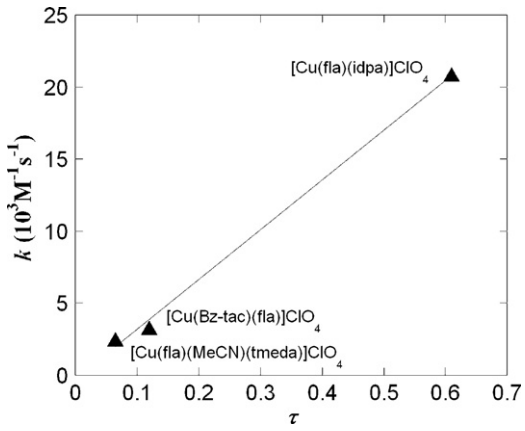

Fig. 10. Reactivity of the ES model complexes in relevance with the geometry of the models (DMF, 0.1 MPa O_2, 120 °C).

latter point is further supported by the mechanism found in case of [Zn(fla)(idpa)]ClO_4 [28] where the valence tautomerism does not function so the coordinated flavonolate anion directly reduces the dioxygen in an intermolecular step yielding the superoxide anion and flavonoxy radical.

3.3.2. Oxygenation reactions of enzyme-substrate (ES) type model complexes. Effect of geometry and co-ligand on the reaction rate and on the chemoselectivity

The bimolecular rate constants for all the oxygenation reactions of the model complexes are orders of magnitude lower than the enzymatic rate constant. The reason is that in the enzyme active site the quercetin is coordinated as a monodentate ligand, in the model systems studied on the other hand, only bidentate coordination of the flavonolate moiety was observed. This leads to an extended delocalisation of π-electrons in the C ring and a rapid equilibrium between the copper(II)–flavonolate and a proposed copper(I)–flavonoxy radical valence tautomer that stabilises the chelate-bound substrate anion (or radical) and makes the oxygenation less favoured than in the case of the singly coordinated substrate. The extent of delocalisation correlates well with the τ value of the five-coordinate model complexes (Fig. 10). This can be rationalised if we suppose that the delocalisation decreases changing from SPY to TBPY geometries (*i.e.* the ΔCu–O_{fla} increases). As a consequence, one observes higher rates for the oxygenation of the models bearing TBPY geometry.

As it is seen, model complexes cannot approximate the efficiency of the FDO enzymes (K_M = 0.0052 M for FDO from *A. flavus* [4], or 0.019 M from *Penicillium oslonii* [49]). However, when oxygenation of [Cu(fla)(idpa)]ClO_4 is performed in the presence of excess acetate co-ligand [50] the reaction rate is increased dramatically (Fig. 11). The acetate is thought to compete with the 4-CO group of the flavolate ligand for the coordination site, *i.e.* [Cu(fla)(idpa)]ClO_4 is transformed to [Cu(fla)(idpa)(OAc)]. This results in the weakening of the chelate-effect regarding the substrate, thus accelerating its oxidation. Moreover, when bulky triphenylacetate is added to the complex, the effect is one order of magnitude greater (Fig. 11) [51]. Although electronic releasing substituents on the flavonolate ligand were shown somewhat to enhance the reaction rate [11], this effect is incommensurable with the rate enhancing effect of the carboxylate co-ligands, especially of the bulky triphenylacetate. In conclusion, steric hindrance of the added co-ligand is thought to be the governing factor in the oxygenation of flavonolate complexes that renders monodentate coordination of the flavonol to the copper, which is less stable than the bidentate coordination. Since the electron density on the C2 atom of the flavonolate moiety is higher when it is only weakly coordinated to

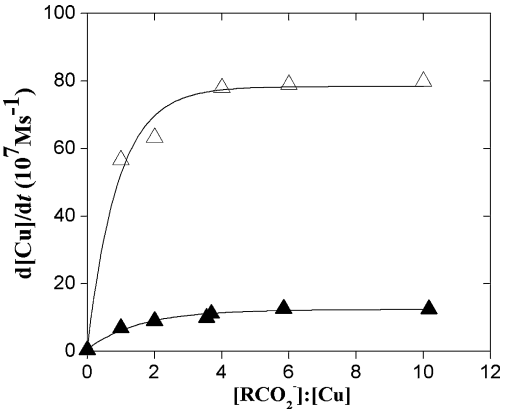

Fig. 11. Rate of dioxygenation of the [Cu(fla)(idpa)]ClO_4 model complex. Effect of the added carboxylate co-ligands (R = Ph_3C (△); R = CH_3 (▲); [Cu] = 5.2×10^{-4} M, DMF, 0.1 MPa O_2, 100 °C).

the metal, direct electron transfer from the activated flavonolate to dioxygen becomes viable resulting in free superoxide radical production that reacts in further steps with the copper(II) flavonoxy intermediate to yield the enzyme-like product (Fig. 12). Formation of superoxide was proven by adding nitroblue tetrazolium (NBT) to the reaction mixture, where the reduction of the added NBT by $O_2^{\bullet -}$ took place [51] by the enzyme-like oxygenation of [Cu(fla)(idpa)]ClO_4. An analogous reaction pathway without the need of redox cycling of the metal was suggested for the Ni- and Co-containing flavonol 2,4-dioxygenase [11]. The added carboxylate in these model systems helps us to understand the role of the glutamate ligand at the active site of the FDO enzyme that plays a role in positioning the quercetin as a monodentate ligand.

Model complexes with general formula [Cu(fla)$_2$(L)] (L = bpy, tmeda, phen) follow a non-enzymatic reaction pathway [39]. In these reactions (Scheme 4) copper(II) 2-hydroxyphenylglyoxylate is formed through a 1,2-dioxethane intermediate. On the other hand, complexes containing only one fla^- ligand with formula [Cu(fla)(L)$_2$]ClO_4, follow the enzymatic route, but typically with a much lower rate. Kinetic studies, ^{18}O-labelling experiments and product analyses support the mechanistic pathways depicted in Scheme 4. Available kinetic data are summarised in Table 5.

Presumably, the coordination mode and the ligand environment around the copper centre, and the Lewis acidity of the copper ion all influence the chemoselectivity of the oxygenation reaction. Since all complexes are sterically very crowded, discrimination of the intramolecular nucleophilic peroxide group attack between the 4-CO and 3-CO carbon atoms seems to be governed by the different electron densities on the named carbon atoms, which partially depends on the ligand environment.

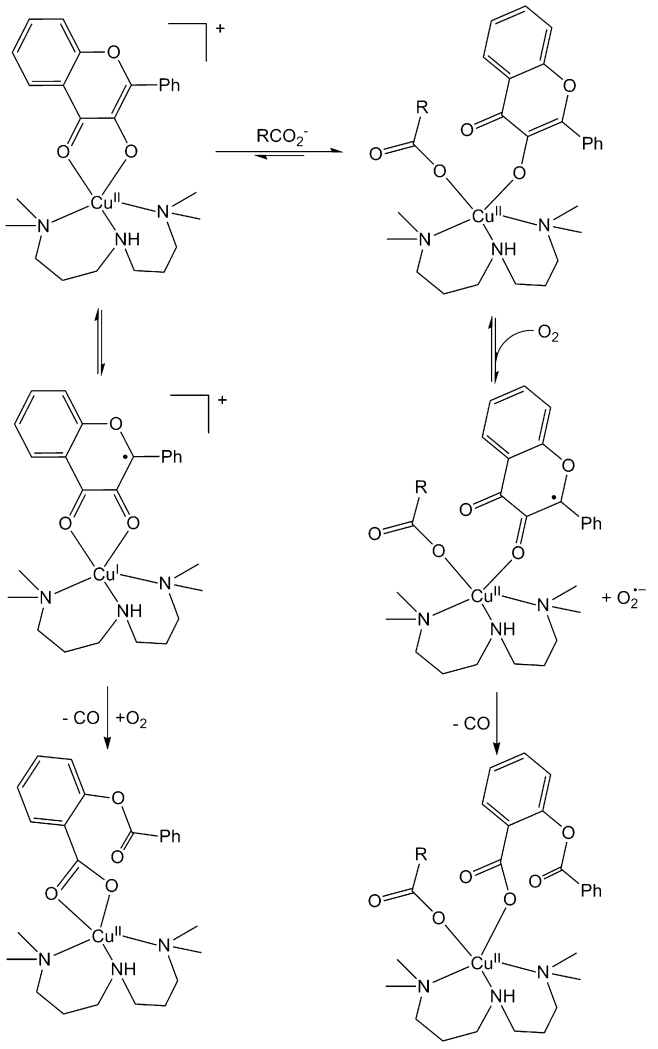

Fig. 12. Mechanistic differences between the oxygenation of [Cu(fla)(idpa)]ClO_4 in the presence and absence of carboxylate co-ligands.

3.4. Oxygenation of flaH derivatives catalysed by model complexes

Several ES and EP models (see in Table 6) function as catalysts in the oxygenation reaction of flaH. The catalyst:substrate ratio ranges from 1:5 to 1:20. All the systems studied produce the enzymatic product *O*-bsH (see Table 6) with satisfactory catalytic activity. The 3N,O-donor set bearing [Cu(bpg)(*O*-bs)], which is a good model for the enzyme form B (Fig. 1) did not exhibit outstanding activity. This is not necessarily contradictory if we note

Table 5
Selected kinetic parameters for the oxygenation reaction of copper–flavonolate complexes.[a].

Complex	T (°C)	k_1 (10^3 M^{-1} s^{-1})	$\Delta\tilde{H}$ (kJ mol^{-1})	$\Delta\tilde{S}$ (J mol^{-1} K^{-1})	Ref.
[Cu(fla)(idpa)]ClO_4	100	6.13 ± 0.16	75 ± 2	−92 ± 3	[52]
	120	20.86 ± 0.94			
[Cu(Bz-tac)(fla)]ClO_4	120	3.31 ± 0.01	–	–	[35]
[Cu(fla)(*i*Pr-tac)]ClO_4	120	1.51 ± 0.01	–	–	[35]
[Cu(fla)$_2$(tmeda)]	80	24.0 ± 1.0	–	–	[39]
[Cu(bpy)(fla)$_2$]	80	20.2 ± 1.0	–	–	[39]
[Cu(fla)$_2$(phen)]	80	95.0 ± 5.0	79 ± 16	−40 ± 44	[39]
[Cu(fla)(phen)$_2$]ClO_4	120	183.0 ± 8.0	–	–	[39]
[Cu(fla)$_2$]	80	15.7 ± 0.8	53 ± 6	−138 ± 11	[32]

[a] All kinetic measurements are performed in DMF solvent. The rate constants are for the processes denoted in Scheme 4. Structures of the abbreviated ligands are shown in Fig. 4. The second-order rate constants and activation parameters are measured at the temperatures indicated above.

Table 6
Oxygenation of flaH in the presence of ES and EP complexes.[a]

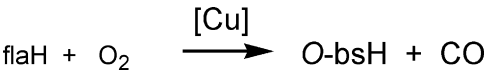

[Cu] catalyst	T (°C)	t (h)	Conversion (%)	Ref.
[Cu(fla)(idpa)]ClO_4	100	8	53	[52]
[Cu(bpg)(*O*-bs)]	100	20	90	[36]
[Cu(Bz-bpa)(*O*-bs)]ClO_4	100	20	91	[36]
[Cu(Bz-6Me$_2$bpa)(*O*-bs)(ClO_4)]	100	20	69	[36]
[Cu(fla)(phen)$_2$]ClO_4	100	10	90	[39]
[Cu(fla)$_2$(phen)]	100	8	100	[39]
[Cu(fla)(ind)]	100	8	17	[39]
[Cu(fla)$_2$(pap)]	100	8	100	[53]
[Cu$_2$(ClO_4)$_2$(fla)$_2$(papH$_2$)]	100	8	87	[53]
[Cu(fla)$_2$]	80	10	78	[54]

[a] Reactions are performed in DMF solvent. Conversion values are for the enzyme-like product *O*-benzoylsalicylic acid and hydrolysed secondary products.

that all the reactions were carried out in DMF, which is a good coordinating solvent itself, and which possibly plays similar role as the carboxylate function, *i.e.* it competes with the substrate for the coordination site and constrains the substrate's monodentate coordination. Another explanation can be the analogous effect of the product *O*-bsH. Consequently, a built-in carboxylate arm in the ligand may play only a minor role in determining the structure of the transient species, and the reaction rate. Interestingly, [Zn(fla)(idpa)]ClO_4 does not catalyse the reaction [28], even at extreme conditions, probably due to stable product–zinc complex formation after the stoichiometric oxygenation of the catalyst. Detailed kinetic studies were carried out on the most efficient catalyst among the 3N-donor ligand containing complexes that aim to model form A of the active site of the FDO enzyme (Fig. 1). These studies on the [Cu(fla)(idpa)]ClO_4–flaH–O_2 system reveal that the rate-determining step is the reaction of the copper flavonolate complex with dioxygen and the free flaH does not play a role in the slow step. Instead, it exchanges the formed *O*-bs$^-$ ligand from the complex in a fast step of the cycle. Thus mechanistically, one cycle corresponds to the oxygenation of the ES model. This mechanism is presumed to apply to the other studied systems, too.

4. Conclusions

Flavonol 2,4-dioxygenase is a metal cofactor dependent enzyme that catalyses the spin-forbidden oxidative decarbonylation of flavonol derivatives into the corresponding depsides using one dioxygen molecule per substrate. The enzyme is thought to circumvent the high energy needed for the spin-forbidden process by the one-electron oxidation of the bound deprotonated substrate yielding a copper(I) flavonoxy radical valence isomer that can react with the triplet dioxygen in a spin allowed step. However, the primary activation of dioxygen stands as an alternative pathway. Studies on [Cu$_2$(μ-O)$_2$], and [Cu$_2$(μ-η^2:η^2O)$_2$] models credibly excluded this alternative as they are inert in their reaction with flaH.

X-ray structural, EXAFS and EPR spectroscopic investigations on the enzymes have clarified that the copper(II) ion is five-coordinate involving a glutamate function, uniquely among copper utilizing oxygenases. Model systems involving multidentate ligands (aimed at mimicking the enzymatic environment) and flavonol coordinated to the copper centre yield enzyme-like products upon oxidation, but only at high temperatures. Structural characterisation of ES type complexes revealed that the substrate forms a stable chelate with the copper centre that explains its sluggish behaviour. Geometry analyses of the ES complexes show that in cases where the (Cu–O_{fla}) bond lengths differ significantly (those with more 5-TBPY character) exhibit higher reactivity. The addition of acetate in high excess further increases the reaction rate significantly. This result supports that the role of glutamate is not the mere deprotonation of the docked substrate, but also directly preventing the chelation of it. Unambiguously, monodentate coordination of the deprotonated substrate to the copper is responsible for the high reactivity towards dioxygen. By the use of radical initiators, or one-electron oxidant and dioxygen, flaH undergoes oxygenation in the enzyme-like reaction. The EPR spectrum of the flavonoxy intermediate, and the dehydro-dimer that is formed in the dioxygen-free reaction proves the spin delocalisation occurring in the B ring of the substrate in accordance with DFT calculations. On this basis, triplet dioxygen might attack the hypothetic copper(I) flavonoxy valence isomer on the high unpaired spin density bearing 2-C sp^3 atom of the flavonoxy moiety, although copper(I) can bind it as well. However, studies summarised in an earlier review on the non-redox metal containing model systems may suggest, that valence tautomerism is not an absolute requirement for FDO-type reactions.

The EP type models provide useful information about the possible coordination modes of the product depside to the copper, since there is no available information about such transient species from the enzymatic systems. The depside is coordinated exclusively *via* the carboxylate function, the ester carbonyl does not interact with the metal. Mono- and bidentate modes alter in the X-rayed models, steric effects seem to have only minor effect, and supposedly donor properties of the ligands determine the structure.

The ES and EP complexes studied, catalyse the enzyme-like oxygenation of flaH, that in contrast with the early models makes the ligand-copper(II)-substrate (or product) complexes useful both as structural and as functional models.

Acknowledgement

Financial support of the Hungarian National Research Fund (OTKA K67871, OTKA K75783 and OTKA PD75360) and COST is gratefully acknowledged.

References

[1] T. Iwashina, J. Plant Res. 113 (2000) 287.
[2] P. Pietta, C. Gardana, A. Pietta, in: C.A. Rice-Evans, L. Packer (Eds.), Flavonoids in Health and Disease, 2nd ed., Marcel Dekker, New York, 2003, p. 43.
[3] F.J. Simpson, N. Narasimhachari, D.W.S. Westlake, Can. J. Microbiol. 9 (1963) 15.
[4] T. Oka, F.J. Simpson, J.J. Child, C. Mills, Can. J. Microbiol. 17 (1971) 111.
[5] E. Schultz, F.E. Engle, J.M. Wood, Biochemistry 13 (1974) 1768.
[6] H.K. Hund, J. Breuer, F. Lingens, J. Huttermann, R. Kappl, S. Fetzner, Eur. J. Biochem. 263 (1999) 871.
[7] D.W.S. Westlake, J.M. Roxburgh, G. Talbot, Nature 189 (1961) 510.
[8] T. Oka, F.J. Simpson, Biochem. Biophys. Res. Commun. 43 (1971) 1.
[9] F. Fusetti, K.H. Schroter, R.A. Steiner, P.I. van Noort, T. Pijning, H.J. Rozeboom, K.H. Kalk, M.R. Egmond, B.W. Dijkstra, Structure 10 (2002) 259.
[10] B. Gopal, L.L. Madan, S.F. Betz, A.A. Kossiakoff, Biochemisty 44 (2005) 193.
[11] H. Merkens, R. Kappl, R.P. Jakob, F.X. Schmid, S. Fetzner, Biochemisty 47 (2008) 12185.
[12] R.A. Steiner, I.M. Kooter, B.W. Dijkstra, Biochemistry 41 (2002) 7955.
[13] T. Oka, F.J. Simpson, H.G. Krishnamurty, Can. J. Microbiol. 18 (1972) 493.
[14] S. Fiorucci, J. Golebiowski, D. Cabrol-Bass, S. Antonczak, Proteins 67 (2007) 961.
[15] R.A. Steiner, W. Meyer-Klaucke, B.W. Dijkstra, Biochemistry 41 (2002) 7963.
[16] S.B. Brown, V. Rajananda, J.A. Holroyd, E.G.V. Evans, Biochem. J. 205 (1982) 239.
[17] R.A. Steiner, K.H. Kalk, B.W. Dijkstra, Proc. Natl. Acad. Sci. U.S.A. 99 (2002) 16625.
[18] I.M. Kooter, R.A. Steiner, B.W. Dijkstra, P.I. van Noort, M.R. Egmond, M. Huber, Eur. J. Biochem. 269 (2002) 2971.
[19] P.E. Siegbahn, Inorg. Chem. 43 (2004) 5944.
[20] S. Fiorucci, J. Golebiowski, D. Carbol-Bass, S. Antonczak, ChemPhysChem 5 (2004) 1726.
[21] A. Nishinaga, T. Tojo, H. Tomita, T. Matsuura, J. Chem. Soc. Perkin Trans. 1 (1979) 2511.
[22] V. Rajananda, S.B. Brown, Tetrahedron Lett. 22 (1981) 4331.
[23] L. Barhács, J. Kaizer, G. Speier, J. Org. Chem. 65 (2000) 3449.
[24] T. Matsuura, H. Matsushima, R. Nakashima, Tetrahedron 26 (1970) 435.
[25] M.M.A. El-Sukkary, G. Speier, J. Chem. Soc. Chem. Commun. (1981) 745.
[26] J. Kaizer, É. Balogh-Hergovich, M. Czaun, T. Csay, G. Speier, Coord. Chem. Rev. 250 (2006) 2222.
[27] É. Balogh-Hergovich, G. Speier, J. Org. Chem. 66 (2001) 7974.

[28] L. Barhács, J. Kaizer, G. Speier, J. Mol. Catal. A: Chem. 172 (2001) 117.
[29] G. Speier, V. Fülöp, L. Párkányi, J. Chem. Soc. Chem. Commun. (1990) 512.
[30] É. Balogh-Hergovich, J. Kaizer, G. Speier, V. Fülöp, L. Párkányi, Inorg. Chem. 38 (1999) 3787.
[31] G. Speier, in: K.D. Karlin, Z. Tyeklár (Eds.), Bioinorganic Chemistry of Copper, Chapman and Hall, New York, 1992.
[32] É. Balogh-Hergovich, J. Kaizer, G. Speier, G. Argay, L. Párkányi, J. Chem. Soc. Dalton Trans. (1999) 3847.
[33] L.M. Bellamy, Ultrarot-Spektrum und chemische Konstitution, Dr. D. Steinkopff Verlag, Darmstadt, 1966, p. 12.
[34] É. Balogh-Hergovich, J. Kaizer, G. Speier, G. Huttner, L. Zsolnai, Inorg. Chim. Acta 304 (2000) 72.
[35] J. Kaizer, J. Pap, G. Speier, L. Párkányi, Eur. J. Inorg. Chem. (2004) 2253.
[36] J. Kaizer, Sz. Góger, G. Speier, M. Reglier, M. Giorgi, Inorg. Chem. Commun. 9 (2006) 251.
[37] J. Kaizer, J. Pap, G. Speier, M. Reglier, M. Giorgi, Trans. Met. Chem. 29 (2004) 630.
[38] É. Balogh-Hergovich, J. Kaizer, G. Speier, G. Huttner, A. Jacobi, Inorg. Chem. 39 (2000) 4224.
[39] É. Balogh-Hergovich, J. Kaizer, J. Pap, G. Speier, G. Huttner, L. Zsolnai, Eur. J. Inorg. Chem. (2002) 2287.
[40] I. Lippai, unpublished work.
[41] I. Lippai, G. Speier, G. Huttner, L. Zsolnai, Acta Crystallogr. Sect. C 53 (1997) 1547.
[42] J. Kaizer, J. Pap, G. Speier, L. Párkányi, Z. Krist, New Cryst. Struct. 219 (2004) 141.
[43] J.A. Halfen, S. Mahapatra, E.C. Wilkinson, S. Kaderli, V.G. Young Jr., L. Que Jr., A.D. Zuberbühler, W.B. Tolman, Science 271 (1996) 1397.
[44] W.B. Tolman, Acc. Chem. Res. 30 (1997) 227.
[45] S. Mahapatra, J.A. Halfen, E.C. Wilkinson, L. Que Jr., W.B. Tolman, J. Am. Chem. Soc. 115 (1994) 9785.
[46] E.A. Lewis, W.B. Tolman, Chem. Rev. 104 (2004) 1047.
[47] J. Kaizer, I. Ganszky, G. Speier, A. Rockenbauer, L. Korecz, M. Giorgi, M. Reglier, S. Antonczak, J. Inorg. Biochem. 101 (2007) 893.
[48] J. Kaizer, G. Speier, J. Mol. Catal. A: Chem. 171 (2001) 33.
[49] S. Tranchimand, G. Ertel, V. Gaydou, C. Gaudin, T. Tron, G. Iacazio, Biochimie 90 (2008) 781.
[50] É. Balogh-Hergovich, J. Kaizer, G. Speier, J. Mol. Catal. A: Chem. 206 (2003) 83.
[51] J.S. Pap, unpublished work.
[52] L. Barhács, J. Kaizer, J. Pap, G. Speier, Inorg. Chim. Acta 320 (2001) 83.
[53] É. Balogh-Hergovich, J. Kaizer, G. Speier, Inorg. Chim. Acta 256 (1997) 9.
[54] É. Balogh-Hergovich, J. Kaizer, G. Speier, J. Mol. Catal. A: Chem. 159 (2000) 215.